RMIT UNIVERSITY

Thank you for downloading this document from the RMIT Research Repository.

The RMIT Research Repository is an open access database showcasing the research outputs of RMIT University researchers.

RMIT Research Repository: http://researchbank.rmit.edu.au/

Citation:

Lynagh, T, Cromer, B, Dufour, V and Laube, B 2014, 'Comparative pharmacology of flatworm and roundworm glutamate-gated chloride channels: Implications for potential anthelmintics', International Journal for Parasitology: Drugs and Drug Resistance, vol. 4, no. 3, pp. 244-255.

See this record in the RMIT Research Repository at:

https://researchbank.rmit.edu.au/view/rmit:29395

Version: Published Version

Copyright Statement:

© 2014 The Authors. Published by Elsevier Ltd. on behalf of Australian Society for Parasitology Inc. This is an open access article under the CC BY-NC-ND license (http://creativecommons.org/licenses/by-nc-nd/3.0/).

Link to Published Version:

http://dx.doi.org/10.1016/j.ijpddr.2014.07.004

PLEASE DO NOT REMOVE THIS PAGE

International Journal for Parasitology: Drugs and Drug Resistance 4 (2014) 244–255

Contents lists available at ScienceDirect

International Journal for Parasitology: Drugs and Drug Resistance

journal homepage: www.elsevier.com/locate/ijpddr

Comparative pharmacology of flatworm and roundworm glutamate-gated chloride channels: Implications for potential anthelmintics

Timothy Lynagh [a,*], Brett A. Cromer [b], Vanessa Dufour [c], Bodo Laube [a]

[a] Neurophysiology and Neurosensory Systems, Technical University of Darmstadt, 64287 Darmstadt, Germany
[b] Health Innovations Research Institute and School of Medical Sciences, RMIT University, Bundoora, Victoria 3083, Australia
[c] Centre for Host–Parasite Interactions, Institute of Parasitology, McGill University – MacDonald Campus, Sainte-Anne-de-Bellevue, Québec H9X 3V9, Canada

ARTICLE INFO

Article history:
Available online 10 August 2014

Keywords:
GluCl
Anthelmintic
Schistosomiasis
Propofol
Thymol
Binding site

ABSTRACT

Pharmacological targeting of glutamate-gated chloride channels (GluCls) is a potent anthelmintic strategy, evidenced by macrocyclic lactones that eliminate numerous roundworm infections by activating roundworm GluCls. Given the recent identification of flatworm GluCls and the urgent need for drugs against schistosomiasis, flatworm GluCls should be evaluated as potential anthelmintic targets. This study sought to identify agonists or modulators of one such GluCl, SmGluCl-2 from the parasitic flatworm *Schistosoma mansoni*. The effects of nine glutamate-like compounds and three monoterpenoid ion channel modulators were measured by electrophysiology at SmGluCl-2 recombinantly expressed in *Xenopus laevis* oocytes. For comparison with an established anthelmintic target, experiments were also performed on the AVR-14B GluCl from the parasitic roundworm *Haemonchus contortus*. L-Glutamate was the most potent agonist at both GluCls, but L-2-aminoadipate, D-glutamate and D-2-aminoadipate activated SmGluCl-2 (EC_{50} 1.0 ± 0.1 mM, 2.4 ± 0.4 mM, 3.6 ± 0.7 mM, respectively) more potently than AVR-14B. Quisqualate activated only SmGluCl-2 whereas L-aspartate activated only AVR-14B GluCls. Regarding the monoterpenoids, both GluCls were inhibited by propofol, thymol and menthol, SmGluCl-2 most potently by thymol (IC_{50} 484 ± 85 μM) and least potently by menthol (IC_{50} > 3 mM). Computational docking suggested that agonist and inhibitor potency is attributable to particular interactions with extracellular or membrane-spanning amino acid residues. These results reveal that flatworm GluCls are pharmacologically susceptible to numerous agonists and modulators and indicate that changes to the glutamate γ-carboxyl or to the propofol 6-isopropyl group can alter the differential pharmacology at flatworm and roundworm GluCls. This should inform the development of more potent compounds and in turn lead to novel anthelmintics.
© 2014 The Authors. Published by Elsevier Ltd. on behalf of Australian Society for Parasitology Inc. This is an open access article under the CC BY-NC-ND license (http://creativecommons.org/licenses/by-nc-nd/3.0/).

1. Introduction

Flatworm parasites are responsible for an astounding disease burden in the developing world. This is exemplified by blood flukes that currently inflict schistosomiasis on hundreds of millions of people (Gryseels et al., 2006; King, 2010). The disease can be deadly but in most cases causes a prolonged morbidity (van der Werf et al., 2003; King et al., 2005) that is clearly associated with oppressive poverty in the affected societies (King, 2010). Treatment of schistosomiasis relies largely on the drug praziquantel, which has been very successful (Doenhoff et al., 2008). A refractory period in juvenile flukes (Pica-Mattoccia and Cioli, 2004; Botros et al., 2005), however, likely renders praziquantel ineffective in areas of high transmission (Gryseels et al., 2001; Doenhoff et al., 2008), and perhaps more alarmingly, very few drugs are available as alternative treatments (Thetiot-Laurent et al., 2013). There is thus a great need for new anthelmintics for schistosomiasis (Caffrey and Secor, 2011; Thetiot-Laurent et al., 2013).

Abbreviations: ECD, extracellular domain; *cis*-ACBD, *cis*-1-aminocyclobutane-1,3-dicarboxylate; GABA, γ-aminobutyric acid; $GABA_AR$, type A γ-aminobutyric acid receptor; GluCl, glutamate-gated chloride channel; GlyR, glycine receptor; iGluR, (tetrameric) ionotropic glutamate receptor; pLGIC, pentameric ligand-gated ion channel (or Cys-loop receptor); TMD, transmembrane domain.

* Corresponding author. Current address: Center for Biopharmaceuticals, Department of Drug Design and Pharmacology, University of Copenhagen, Jagtvej 160, 2100 Copenhagen, Denmark. Tel.: +45 35321535.

E-mail addresses: tpl@sund.ku.dk (T. Lynagh), brett.cromer@rmit.edu.au (B.A. Cromer), vanessa.dufour@mail.mcgill.ca (V. Dufour), laube@bio.tu-darmstadt.de (B. Laube).

http://dx.doi.org/10.1016/j.ijpddr.2014.07.004
2211-3207/© 2014 The Authors. Published by Elsevier Ltd. on behalf of Australian Society for Parasitology Inc.
This is an open access article under the CC BY-NC-ND license (http://creativecommons.org/licenses/by-nc-nd/3.0/).

One of the most effective anthelmintic targets thus far is the glutamate-gated chloride channel (GluCl) of roundworms, a membrane-bound receptor-channel in neuronal and muscle cells, where it mediates an inhibitory chloride current in response to neurotransmitter binding (Wolstenholme, 2012). It is a uniquely invertebrate member of the pentameric ligand-gated ion channel (pLGIC) family, also known as Cys-loop receptors. GluCls are closely related to mammalian glycine receptor (GlyR) and Type A GABA receptor ($GABA_AR$) pLGICs (Dent, 2006). The potency of the GluCl as an anthelmintic target is demonstrated by the widely used macrocyclic lactone, ivermectin, which binds with high affinity to the membrane-spanning domain of roundworm GluCls, irreversibly activating a chloride current (Dent et al., 2000; Lynagh and Lynch, 2012b). In the parasitic nematode, this depresses motor, sensory and secretory systems (Kass et al., 1980; Perry, 2001; Moreno et al., 2010), which serves to eliminate nematode infections from millions of humans suffering from diseases such as river blindness and lymphatic filariasis (Omura, 2008).

Despite their successful treatment of numerous roundworm infections, macrocyclic lactones are largely ineffective against flatworms, with practically no activity in flukes (Shoop et al., 1995) and relatively low potency at tapeworms (Campbell et al., 1983; Perez-Serrano et al., 2001). Consequently, flatworm GluCls did not appear relevant as anthelmintic targets. Indeed, it was unclear if GluCls were even present in flatworms until very recently, when four GluCl subunits, SmGluCl1-4, were isolated from *Schistosoma mansoni* (Dufour et al., 2013). SmGluCl-2 and -3 form homomeric channels that are not activated by macrocyclic lactones, but their robust responses to L-glutamate, together with the conservation of similar transcripts in other flatworms (Dufour et al., 2013), suggest that their pharmacological modulation could constitute a novel treatment for a wide range of flatworm parasites. Furthermore, these channels reveal similarities with roundworm GluCls, suggesting that it may be possible for certain compounds to target both roundworm and flatworm GluCls, potentially leading to anthelmintics of an unprecedented broad spectrum. A recent high-resolution structure of a homomeric roundworm GluCl from *Caenorhabditis elegans* has outlined general pLGIC architecture and precisely defined the binding sites for glutamate and ivermectin (Hibbs and Gouaux, 2011). Glutamate binds in the extracellular domain (ECD), between principal Loops A, B and C of one subunit and complementary Loops D, E, F and G of an adjacent subunit. Ivermectin occupies a cavity between adjacent subunits in the transmembrane domain (TMD), which in mammalian pLGICs contains binding sites for various modulators of agonist-induced activation.

In the present work, a flatworm GluCl was examined as a pharmacological target in comparison to a roundworm GluCl that is already established as a useful anthelmintic target. To this end, the SmGluCl-2.1 from *S. mansoni* and the AVR-14B GluCl from *Haemonchus contortus* were recombinantly expressed in *Xenopus laevis* ooctyes, and both channels were tested for activation or modulation by several compounds. These GluCls were selected according to their qualities representative of other GluCls from the respective phyla: SmGluCl-2.1 shows robust responses to glutamate and is phylogenetically similar to numerous other flatworm GluCls, both trematode and cestode (Dufour et al., 2013); AVR-14B is highly conserved in parasitic roundworms (Beech et al., 2010), has typical roundworm GluCl ivermectin sensitivity (McCavera et al., 2009) and is a verified nematicidal target (Glendinning et al., 2011). Compounds were selected due to their analogy with known agonists that bind to the ECD or modulators that bind to the TMD of other pLGICs. Several compounds acted as moderate-to-low affinity agonists or inhibitors, suggesting sites for potential anthelmintic compounds are possessed by flatworm and roundworm GluCls alike.

2. Materials and methods

2.1. Drugs, chemicals, reagents

S. mansoni SmGluCl-2.1 (hereafter referred to as SmGluCl-2; (Dufour et al., 2013); in the pT7TS vector) and *H. contortus* AVR-14B (in pT7TS) cDNAs were kind donations from Professor Timothy Geary (Institute of Parasitology, McGill University, Montréal, Canada) and Professor Adrian Wolstenholme (Department of Infectious Diseases, University of Georgia, Athens, GA, USA), respectively. The AVR-14B Arg95Ala mutant cDNA was constructed using mutagenesis primers synthesized by Eurofins MWG Operon (Ebersberg, Germany) and the Quikchange II XL Site-Directed Mutagenesis kit (Agilent Technologies, Böblingen, Germany), and it was confirmed by DNA sequencing (Eurofins MWG Operon). XbaI was purchased from Fisher Scientific Germany GmbH (Schwerte, Germany). The mMESSAGE mMACHINE T7 Kit for transcription was purchased from Life Technologies GmbH (Darmstadt, Germany). Chemicals and drugs were purchased from AppliChem GmbH (Darmstadt, Germany), Carl Roth GmbH (Karlsruhe, Germany), Sigma–Aldrich (Munich, Germany) or Tocris Bioscience (R&D Systems GmbH, Wiesbaden-Nordenstadt, Germany).

2.2. Electrophysiological experiments

X. laevis oocytes were obtained, defolliculated and stored as previously described (Lynagh et al., 2013). After cDNA linearization with XbaI and cRNA synthesis with the mMESSAGE mMACHINE T7 kit, 4 ng cRNA was injected into defolliculated oocytes, and oocytes were stored in frog Ringer's solution (96 mM NaCl, 2 mM KCl, 1 mM $CaCl_2$, 1 mM $MgCl_2$, 5 mM HEPES; pH 7.4 with NaOH; 50 μg/mL gentamycin). 2–5 days later, oocytes were transferred to a recording chamber and constantly perfused with bath solution (115 mM NaCl, 1 mM KCl, 1.8 mM CaCl2, 10 mM HEPES; pH 7.4 with NaOH). Oocytes were two electrode voltage-clamped at −70 mV with micropipettes filled with 3 M KCl. Currents were filtered at 200 Hz and sampled at 1000 Hz with a Geneclamp 500B amplifier, Digidata 1322A interface and Clampex software (Molecular Devices, Sunnyvale, CA, USA). Currents were measured in response to increasing concentrations of L-glutamate or other agonists, each dissolved in bath solution. Modulation of L-glutamate-induced currents was tested by co-applying increasing concentrations of the compound in question with the half maximal effective concentration (EC_{50}) of L-glutamate.

2.3. Amino acid sequence alignments, homology modeling and dockings

Amino acid alignments were performed with ClustalX2 (Larkin et al., 2007). To estimate the binding sites for the compounds tested, comparative models of SmGluCl-2 and AVR-14B were built on the template crystal structure of the *C. elegans* GLC-1 GluCl (PDB entry 3RIF; (Hibbs and Gouaux, 2011)) using Modeller (Eswar et al., 2006). Computational docking was performed with AutoDock Vina including flexible side chains (Trott and Olson, 2010). Glutamate and related compounds were docked to each model within a cube of sides 20 Å encompassing the L-glutamate binding site identified in the *C. elegans* GLC-1 GluCl (Hibbs and Gouaux, 2011). Modulators were docked to a $28 \times 28 \times 25$ Å volume in the extracellular half of the TMD, including intrasubunit cavities of two adjacent

subunits and an intersubunit cavity between two subunits, traversing from the membrane to the channel pore between two M2 helices. Initial docking at this second site was performed with fixed side chains and then repeated with flexible side chains surrounding the preferred intersubunit site.

2.4. Data analysis and statistical procedures

All data were analyzed in Prism4 software (GraphPad Software Inc., San Diego, CA, USA). For calculation of EC_{50} and n_H values, current responses to agonists were plotted against log agonist concentration and fit with non-linear regression. Mean ± s.e.m. from at least 3 individual experiments are reported. Maximal agonist-induced currents (I_{max}) in tables and figures were normalized to the mean maximal L-glutamate-induced current, which is itself reported in the table. For the agonist dose–response curves in the figures, data points are the mean ± s.e.m. for the indicated number of experiments, and the curves are an illustrative fit to these points. For modulation of EC_{50} L-glutamate-induced currents, peak current (cyan dashed lines in Fig. 5A and B) in the combined presence of modulator and EC_{50} L-glutamate, as a percentage of peak current in the presence of EC_{50} L-glutamate alone, was plotted against log concentration of modulator. IC_{50} and n_H values were also calculated with non-linear regression, and points and curves in figures were generated as for agonists. In quantitating desensitization, time taken for current to halve ($t_{1/2}$) was calculated for maximal and half-maximal L-glutamate-induced currents. Mean ± s.e.m. $t_{1/2}$ values were compared with paired (maximal vs. half-maximal for each channel) or unpaired (SmGluCl-2 vs. AVR-14B channels) *t* tests (Prism4).

3. Results

3.1. Glutamate-like compounds activate S. mansoni SmGluCl-2 and H. contortus AVR-14B GluCls

In testing compounds for activity at SmGluCl-2 and AVR-14B GluCls, we first considered several compounds with structural analogy to L-glutamate (Fig. 1), reasoning that these might also act as agonists. To this end, L-glutamate, D-glutamate, L-2-aminoadipate, D-2-aminoadipate, quisqualate, L-aspartate, *cis*-1-aminocyclobutane-1,3-dicarboxylate (*cis*-ACBD), GABA, and glycine were all applied at increasing concentrations to *X. laevis* oocytes injected with SmGluCl-2 or AVR-14B cRNA and current responses were recorded with two-electrode voltage clamp electrophysiology.

In SmGluCl-2-expressing oocytes, currents were activated dose-dependently by L-glutamate, D-glutamate, L-2-aminoadipate, D-2-aminoadipate and quisqualate (Fig. 2A and D). Currents decreased in the continued presence of each agonist (Fig. 2A), indicating that desensitization is a common feature of agonist activity at SmGluCl-2. L-glutamate was by far the most potent agonist, with an EC_{50} value of 24 ± 3 μM, 1.5 orders of magnitude lower than that of the next-most potent agonist (Table 1) and similar to that previously reported for SmGluCl-2 (Dufour et al., 2013). The time taken for ~EC_{50} and saturating L-glutamate-induced currents to decay to half-maximal amplitude was 9.3 ± 1.1 s and 5.3 ± 0.8 s, respectively ($n = 4$). These values are significantly different ($P < 0.01$; paired t test), indicating that desensitization is faster at higher agonist concentrations.

L-2-aminoadipate and D-glutamate were both full agonists at SmGluCl-2, with EC_{50} values of 1.0 ± 0.1 mM and 2.4 ± 0.4 mM and maximal currents (I_{max} values) that equated to 93 ± 6% and 100 ± 6% that activated by L-glutamate, respectively (absolute I_{max} values were not significantly different from L-glutamate when analyzed with paired *t*-test). D-2-aminoadipate, with an EC_{50} of 3.6 ± 0.7 mM, activated currents with an I_{max} of 86 ± 3% that of L-glutamate, indicating that the D-isomer is a partial agonist at the SmGluCl-2 (absolute I_{max} values were significantly less than L-glutamate at individual oocytes, $n = 4$, $P < 0.05$, paired *t*-test). Quisqualate, which differs from the other L-glutamate analogues in the presence of a 1,2,4-oxadiazolidine-3,5-dione instead of a carboxyl terminal (Fig. 1), at the highest concentration tested (10 mM) activated currents equivalent to 28 ± 5% the L-glutamate I_{max} (Fig. 2A). No currents were activated by L-aspartate, GABA, glycine (each at concentrations up to 100 mM) or *cis*-ACBD (at concentrations up to 10 mM). Numerous compounds bind to but do not activate pLGICs, thus acting as competitive antagonists of channel activation. We tested this possibility for L-aspartate, GABA, glycine and *cis*-ACBD at the SmGluCl-2 by co-applying these compounds at 100 mM (or 10 mM for *cis*-ACBD) with submaximal concentrations of L-glutamate. No antagonism of current responses to L-glutamate was observed for any of the compounds (data not shown), indicating that the absence of agonist effects is indeed due to low binding affinity.

We next examined the agonist effects of these compounds at the *H. contortus* AVR-14B GluCl, in order to establish if similar sites for these compounds are conserved in roundworm and flatworm GluCls. Like the SmGluCl-2, the AVR-14B GluCl was activated by several of the tested compounds, with each agonist causing significant desensitization (Fig. 2B). Again, L-glutamate was the most potent agonist, with an EC_{50} of 21 ± 6 μM, similar to previous

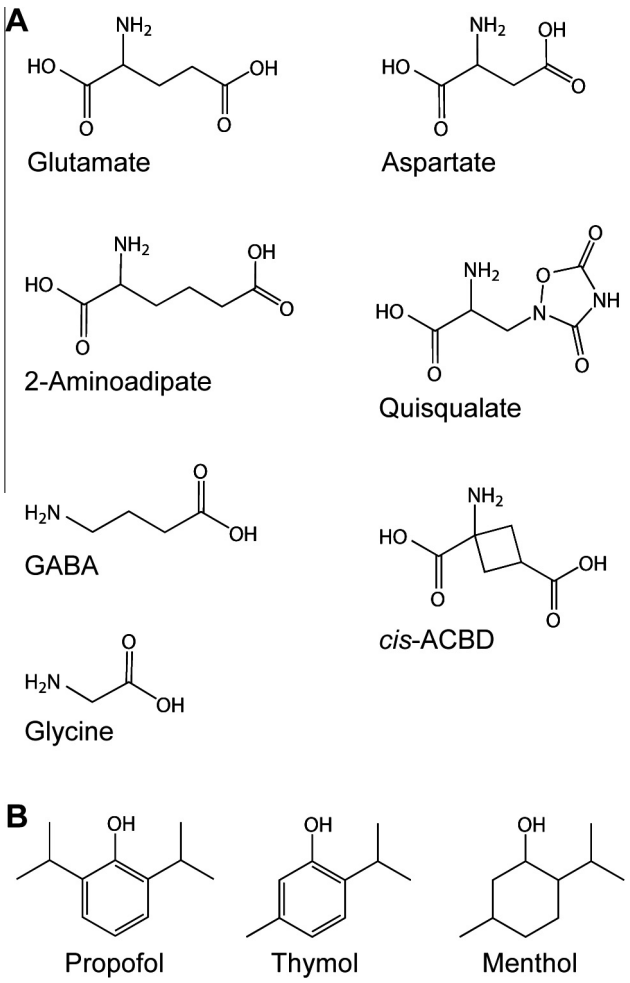

Fig. 1. Compounds tested for effects at GluCls. (A) Compounds tested for agonist effects. L- and D-isomers of glutamate and 2-aminoadipate were tested. (B) Compounds tested for modulatory effects.

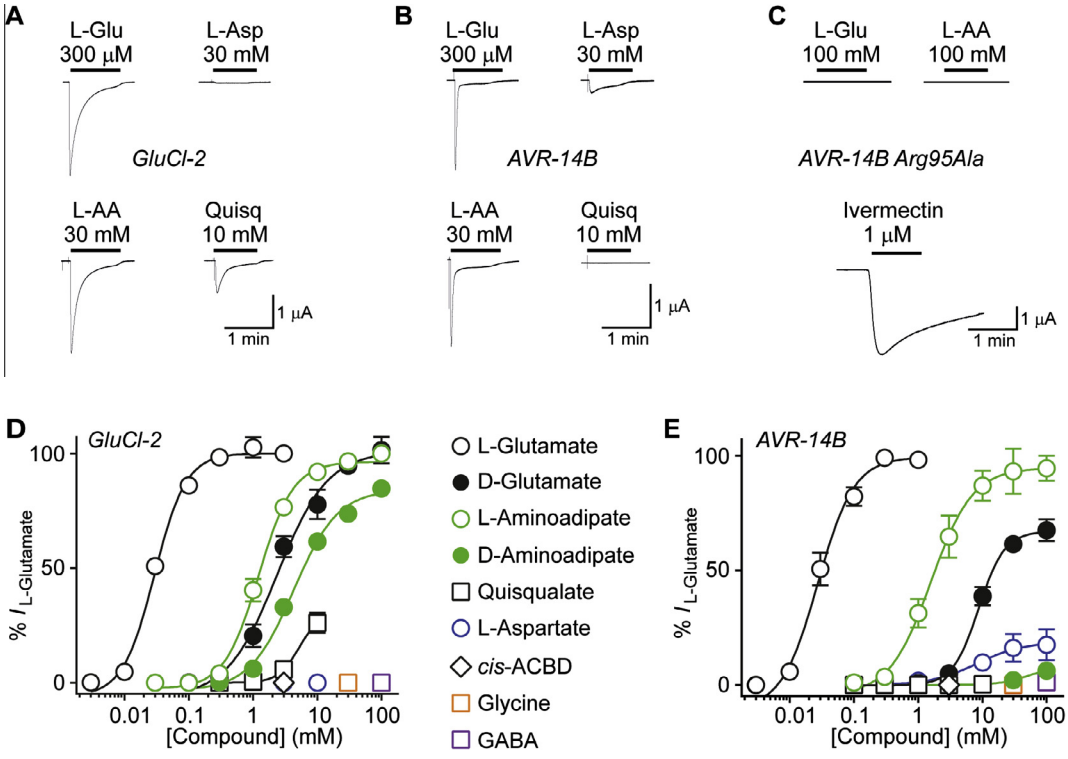

Fig. 2. Agonist effects of L-glutamate-like compounds. (A–C) Typical current responses to selected compounds at oocytes expressing wild-type SmGluCl-2 (A), wild-type AVR-14B (B), or mutant Arg95Ala AVR-14B. *L-Glu*, L-glutamate; *L-Asp*, L-aspartate; *L-AA*, L-aminoadipate; *Quisq*, quisqualate. (D,E) Current amplitude normalized to maximum L-glutamate-induced current (% $I_{\text{L-Glutamate}}$; mean ± s.e.m. $n = 3–5$) in response to increasing concentrations of all compounds at wild-type SmGluCl-2 (D) and AVR-14B (E). Mean data points are fit with non-linear regression for display. Fits for individual experiments were used to calculate the parameters in Table 1.

reports (McCavera et al., 2009). The time taken for ~EC_{50} and saturating L-glutamate-induced currents to decay to half-maximal amplitude was 3.4 ± 0.6 s and 2.8 ± 0.7 s, respectively ($n = 4$). These values are not significantly different from each other (paired *t* test) and both significantly lower than the corresponding values at SmGluCl-2 ($P < 0.01$ for EC_{50} and $P < 0.05$ for saturating; unpaired *t* test). This indicates that desensitization of AVR-14B channels is (1) similar at low and high agonist concentrations and (2) faster than SmGluCl-2 channels.

L-2-aminoadipate also acted as a full agonist (Fig. 2B and E) with an EC_{50} that was two orders of magnitude higher than L-glutamate (Table 1). D-isomers of glutamate and 2-aminoadipate were markedly less potent at the AVR-14B GluCl than at the SmGluCl-2 (compare filled circles in Fig. 2D to filled circles in Fig. 2E), activating currents that equated to only 67 ± 5% and 3 ± 1%, respectively, of the L-glutamate I_{max} at the AVR-14B GluCl. The EC_{50} of D-glutamate was 8.8 ± 0.6 mM, more than two orders of magnitude greater than that of L-glutamate. Also in contrast to SmGluCl-2, the AVR-14B GluCl was not activated by 10 mM quisqualate but was robustly activated by L-aspartate as a partial agonist (compare Fig. 2A and B), with an I_{max} of 17 ± 7% that of L-glutamate and an EC_{50} of 8.7 ± 3 mM ($n = 3$). 100 mM GABA, 100 mM glycine and 10 mM *cis*-ACBD activated no current and did not inhibit responses to EC_{50} L-glutamate at the AVR-14B GluCl (data not shown).

Finally, we sought to exclude the possibility that the observed responses to high agonist concentrations were not GluCl-mediated and were mediated by some endogenous oocyte channel. To this end, we tested the effects of agonists at 100 mM on oocytes injected with mutated, Arg95Ala AVR-14B cRNA. This arginine putatively contributes to L-glutamate binding (position 7 in

Table 1
Agonist parameters of L-glutamate analogues at SmGluCl-2 and AVR-14B GluCls.

	SmGluCl-2				AVR-14B GluCl			
	EC_{50} (mM)	n_H	I_{max} (µA or %[a])	*n*	EC_{50} (mM)	n_H	I_{max} (µA or %[a])	*n*
L-glutamate	0.024 ± 0.003	1.8 ± 0.2	3.2 ± 0.6	7	0.021 ± 0.006	1.9 ± 0.2	3.1 ± 0.3	4
D-glutamate	2.4 ± 0.4	1.1 ± 0.1	100 ± 6	3	8.8 ± 0.6	2.3 ± 0.1	67 ± 5	4
L-2-aminoadipate	1.0 ± 0.1	1.7 ± 0.3	93 ± 6	4	2.6 ± 1.0	1.3 ± 0.2	98 ± 2	6
D-2-aminoadipate	3.6 ± 0.7	1.0 ± 0.1	86 ± 3	4	[b]	[b]	4 ± 1	3
L-aspartate	[b]	[b]	1 ± 1	3	8.7 ± 0.3	1.5 ± 0.4	17 ± 7	3
Quisqualate	[c]	[c]	28 ± 5	3	[b]	[b]	0	3
cis-ACBD	[b]	[b]	0	4	[b]	[b]	0	4
GABA	[b]	[b]	0	3	[b]	[b]	0	3
Glycine	[b]	[b]	0	3	[b]	[b]	0	3

[a] Absolute L-glutamate I_{max} reported in µA; all others as percentage of L-glutamate I_{max}.
[b] Inactive.
[c] Current activated by 10 mM quisqualate.

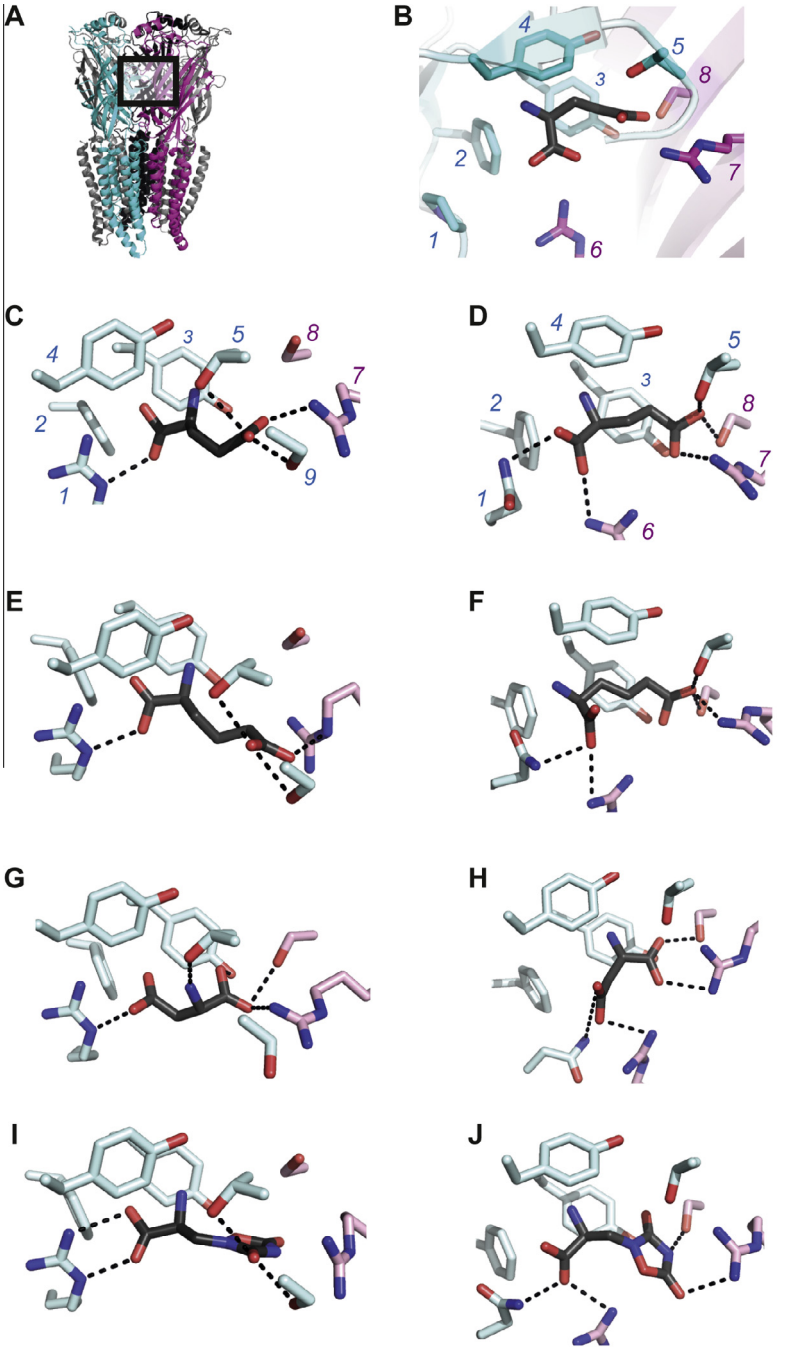

K

	Loop A		Loop B	Loop C		Loop D	Loop E	Loop G
	2	1	3	95	4	7	8	6
GLC-1	PDT	**FF**	**P**N	AS**Y**AY	CTSVT	**NT**--GI**Y**SC	LTL**R**ESW	LY**S**VRI	L**R**T
AVR-14B	PDT	**FF**	**Q**N	AS**Y**AY	CTSKT	**NT**--GE**Y**SC	FTF**R**EEW	LY**S**VRL	L**R**S
GluCl-2	PDL	**FF**	**R**N	GS**Y**GY	CSSGY	**ST**STGQ**Y**TC	LLL**R**QVW	LY**S**QKI	V**L**A

Fig. 3. Simulated dockings to extracellular L-glutamate-binding domain. (A) GLC-1 crystal structure (Protein Database entry 3RIF), viewed from within the membrane plane. Two adjacent subunits are shown in cyan and magenta. (B) Detailed view of boxed area in (A), showing bound L-glutamate molecule and proximal side chains: *1*, Pro93 and *2*, Phe91 in Loop A; *3*, Tyr151 in Loop B; *4*, Tyr200 and *5*, Thr197 in Loop C; *6*, Arg37 in Loop G; *7*, Arg56 in Loop D; and *8*, Ser121 in Loop E (Hibbs and Gouaux, 2011). Part of Loop C in the foreground is removed for clarity. (C–J) dockings of L-glutamate (C and D), L-aminoadipate (EC and F), L-aspartate (GC and H) and quisqualate (IC and J) to homology models of SmGluCl-2 (C, E, G, I) or AVR-14B (D, F, H, J). Dashed lines indicate distances ⩽3.2 Å. Side chains equivalent to those in GLC-1 are numbered as in (B), including an additional serine, *9*, in SmGluCl-2 Loop C (C, E, G, I). (K) Relevant segments from an amino acid alignment of *Caenorhabditis elegans* GLC-1, *Schistosoma mansoni* SmGluCl-2 and *Haemonchus contortus* AVR-14B, indicating the equivalence of the illustrated side chains.

Fig. 3D), and its mutation to alanine should therefore impair agonist-gated currents without affecting functional expression; if oocytes injected with Arg95Ala cRNA showed no response to 100 mM agonist concentrations, this would rule out the contribution of other endogenous channels to current responses. Despite robust Arg95Ala GluCl expression, as evident in ivermectin-activated currents, these oocytes did not respond to 100 mM agonist concentrations (Fig. 2C), confirming that the responses of wild-type cRNA-injected oocytes were indeed mediated directly by GluCls.

3.2. Computational docking to homology model ECDs

L-glutamate binds to GluCls in the ECD at the interface of adjacent subunits (Fig. 3A and B), as illustrated by the crystal structure of the *C. elegans* GLC-1 GluCl in complex with L-glutamate (Hibbs and Gouaux, 2011). To investigate the molecular basis for the differential pharmacology of GluCls, we first built homology models of SmGluCl-2 and AVR-14B GluCls on the *C. elegans* GLC-1 GluCl template (PDB entry 3RIF). SmGluCl-2 and AVR-14B share 30–50% amino acid identity with GLC-1, enabling modeling with a high degree of confidence. Other than a proline/glutamine difference (position "1" in Fig. 3B) in Loop A, all of the key residues that interact with the bound agonist in the 3RIF GLC-1 structure are conserved in AVR-14B. These include two tyrosine residues (positions 3 and 4 in Loops B and C, respectively, in Fig. 3B) in the so-called aromatic box that coordinate the agonist primary amine; threonine, arginine and serine residues (positions 5, 7, and 8 in Loops C, D and E, respectively, in Fig. 3B) that coordinate the agonist γ-carboxyl; and a loop G arginine that coordinates the agonist α-carboxyl in GLC-1 (position 6 in Fig. 3B). There are however some notable differences between SmGluCl-2 and both AVR-14B and GLC-1. Firstly there are two extra residues between the two disulphide-linked cysteines in loop C, as shown in Fig. 3K. In an SmGluCl-2 model built on this alignment, the residues surrounding the agonist, described above, are largely conserved, except for an arginine in place of the Loop A proline/glutamine; an uncharged leucine in place of the loop G arginine that coordinates the agonist γ-carboxyl in GLC-1; and an extra tyrosine from loop C contributing to the aromatic box (Fig. 3K).

To identify potential determinants of differential pharmacology, the ligands tested above were computationally docked to SmGluCl-2 and AVR-14B homology models. The highest ranked docking of L-glutamate to AVR-14B adopted a position similar to that in the *C. elegans* GLC-1 crystal structure, with the agonist amino nitrogen in close proximity to the two aromatic box tyrosines from Loops B and C of the principal face (Fig. 3B and D) and forming an H-bond to the loop-B backbone (not shown). The L-glutamate γ-carboxyl formed a salt-bridge with the Loop D arginine of the AVR-14B complementary face and similar H-bonds with the Loop C threonine and loop E serine side chains (Fig. 3D). Likewise, the L-glutamate α-carboxyl formed a salt-bridge with the Loop G arginine at the "bottom" of the AVR-14B site, similar to that in the GLC-1 structure. Conversely, when docked to SmGluCl-2, the L-glutamate α-carboxyl formed a salt-bridge with loop A arginine side chain, in the absence of a Loop G arginine (Fig. 3C). The altered position of this coordinating charge, from the "bottom" (Fig. 3D) in AVR-14B to the "left" ("Fig. 3C) of the agonist site in SmGluCl-2, may be a significant factor in changes to other agonist-receptor interactions. The docked primary amine shifts more to the "right" in SmGluCl-2, removing the H-bond to the loop B backbone and shifting the most apparent cation-π bond from a Loop C tyrosine to a loop B tyrosine. Although the L-glutamate γ-carboxyl again formed a salt-bridge with the Loop D arginine and an H-bond with the Loop C threonine, the H-bond to the Loop E serine was replaced by one with a Loop C serine. The additional tyrosine in SmGluCl-2 loop C, not present in AVR-14B (Fig. 3K; omitted for clarity from other illustrations), forms apparent hydrophobic interactions with β- and γ-carbon atoms of L-glutamate that may stabilize this orientation of bound agonist.

Other ligands that activated both channels showed reasonably similar binding modes to L-glutamate at each model, including the full agonist L-2-aminoadipate (Fig. 3E and F) but with some modifications to accommodate the longer agonist. In general, D-isomers docked best in a flipped orientation (not shown), such that the agonist α-carboxyl interacts with the complementary face Loop D arginine and the α-amino nitrogen can form a cation-π interaction with the Loop B tyrosine even in the AVR-14B site. Slightly lower-ranked docks of D-glutamate to SmGluCl-2 showed similar receptor-agonist interactions to L-glutamate, apparently better accommodating the altered stereochemistry of D-glutamate than AVR-14B, perhaps underlying the lower L/D selectivity of SmGluCl-2. In dockings of L-aspartate to both channels (Fig. 3G and H), agonist carboxyl groups interacted with the same positively charged side chains but, relative to L-glutamate, the two carboxyl groups were effectively swapped, flipping the agonist such that the α-carboxyl was oriented towards the complementary face. This arrangement alters many interactions, notably shifting major cation-π interactions from the Loop C tyrosine to the Loop B tyrosine in AVR-14B and away from any aromatic side chain in SmGluCl-2, perhaps explaining the selective agonist activity of L-aspartate at the AVR-14B GluCl. Dockings of quisqualate appeared similar at both receptors, although an interaction between the agonist oxodiazolidine-3,5-dione terminal and the Loop C threonine side chain was lacking in the AVR-14B (Fig. 3I,J), perhaps explaining its selective activity at the

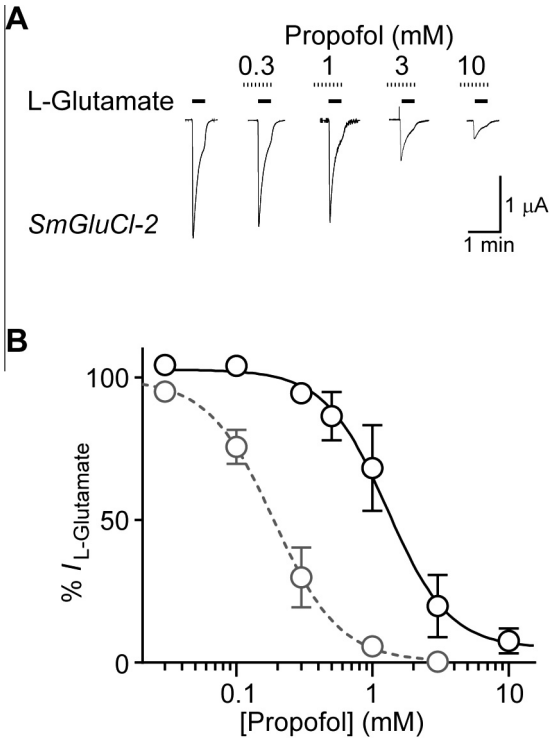

Fig. 4. Propofol inhibition of SmGluCl-2. (A) Typical current responses to EC_{50} L-glutamate in the presence of increasing concentrations of propofol at an oocyte expressing SmGluCl-2. (B) Current responses at SmGluCl-2-expressing oocytes (black circles) to EC_{50} L-glutamate in the presence of propofol at increasing concentrations, normalized to the response in the absence of propofol (% $I_{L\text{-Glutamate}}$; mean ± s.e.m. $n = 5$). Mean data points are fit with non-linear regression for display. Fits for individual experiments were used to calculate the parameters in Table 2. Dashed line/grey circles illustrate the same experiments at AVR-14B-expressing oocytes, from (Lynagh and Laube, 2014).

SmGluCl-2. Glycine and GABA docked poorly to both models, correlating with their lack of activity at both channels.

3.3. Monoterpenoids inhibit SmGluCl-2 and AVR-14B GluCls

It was recently shown that the AVR-14B GluCl contains a TMD binding site for the general anesthetic propofol (2,6-diisopropylphenol), which in the micromolar range inhibits responses to L-glutamate (Lynagh and Laube, 2014). If propofol were to inhibit flatworm GluCls at low concentrations it could constitute a novel anthelmintic lead, and therefore, the SmGluCl-2 was tested for sensitivity to propofol. Responses to EC_{50} L-glutamate were dose-dependently inhibited by propofol (Fig. 4), with an IC_{50} of 1.1 ± 0.4 mM (n = 5). This is higher than the concentrations of propofol required for inhibition of AVR-14B (Fig. 4B) and substantially higher than the concentrations of propofol that enhance human ion channels and induce anesthesia (Franks and Lieb, 1994). Propofol itself is therefore unsuitable as an anthelmintic. However, given that certain propofol derivatives can modulate pLGICs with >1000-fold greater potency than propofol (de la Roche et al., 2012) and that the structurally related monoterpenoids thymol (2-isopropyl-5-methyl-phenol) and menthol (2-isopropyl-5-methyl-phenol) modulate pLGICs (Priestley et al., 2003; Tong and Coats, 2012), we considered that these might modulate the SmGluCl-2 with greater potency than propofol.

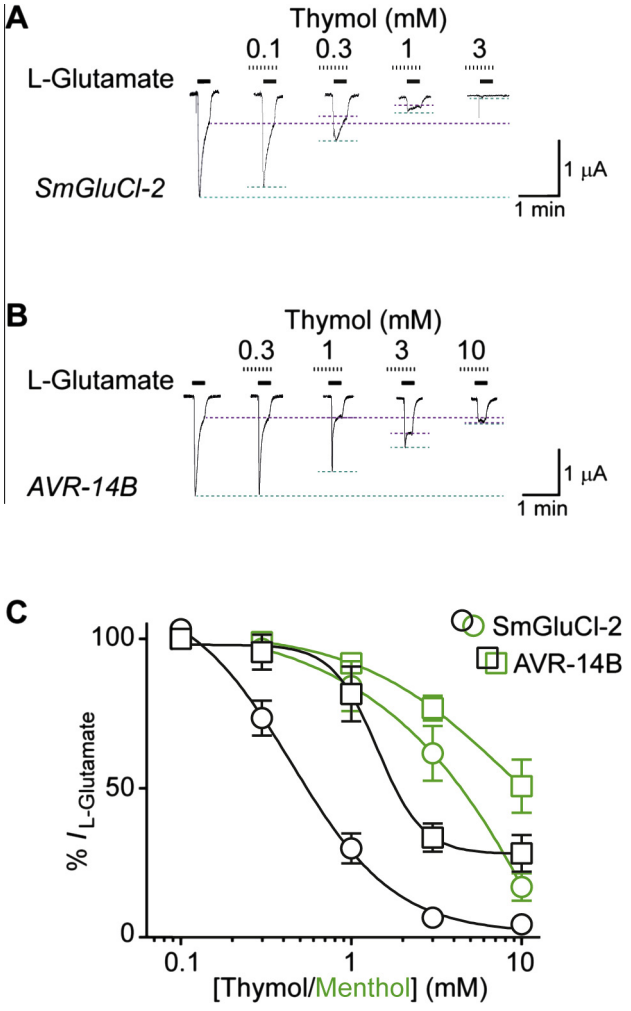

Fig. 5. Thymol and menthol inhibition of GluCls. (A and B) Typical current responses to EC_{50} L-glutamate in the presence of increasing concentrations of thymol at an oocyte expressing SmGluCl-2 (A) or AVR-14B (B). Cyan dashed line indicates peak current responses; purple dashed line indicates current after 30 s agonist application. Note in (B) that 3 mM thymol caused an increase in the current after 30 s agonist application. (C) Peak current responses at SmGluCl-2- and AVR-14B-expressing oocytes to EC_{50} L-glutamate in the presence of thymol or menthol at increasing concentrations, normalized to response in the absence of modulator (% $I_{L\text{-}Glutamate}$; mean ± s.e.m. n = 3–4). Mean data points are fit with non-linear regression for display. Fits for individual experiments were used to calculate the parameters in Table 2.

Thymol dose-dependently inhibited up to 95 ± 4% (n = 4) of the L-glutamate response at the SmGluCl-2 (Fig. 5A), with an IC_{50} value of 484 ± 85 µM (n = 4) that is lower than, but not significantly different from, that of propofol (Table 2). Thymol also inhibited the AVR-14B GluCl (Fig. 5B), but with an IC_{50} value of 1.2 ± 0.2 mM (n = 4), significantly higher than that at the SmGluCl-2 (P < 0.05, unpaired t-test), and to a smaller maximal extent than SmGluCl-2 (P < 0.05, unpaired t-test). The results reported thus far refer to inhibition of the peak current responses to EC_{50} L-glutamate (cyan dashed lines in Fig. 5A and B). Fig. 5B shows that although thymol inhibited peak currents at the AVR-14B GluCl, it actually enhanced the current present after prolonged L-glutamate application (purple dashed lines in Fig. 5B). This effect did not show robust dose-dependency and was not analyzed further. Taken together, these data indicate that thymol is more potent than propofol in inhibiting SmGluCl-2, whereas the converse is true for inhibition of the AVR-14B GluCl. Finally, we tested for inhibition of both GluCls by menthol. Menthol and thymol are identical compounds but for the absence of double bonds in the cyclohexyl backbone of menthol (Fig. 1). Menthol inhibited both GluCls (Fig. 5C), with 10 mM menthol (highest concentration tested) causing 83 ± 5% (n = 3) and 49 ± 9% (n = 4) inhibition of EC_{50} L-glutamate responses at Sm-GluCl-2 and AVR-14B GluCls, respectively. Menthol is thus substantially less potent than propofol or thymol at inhibiting either GluCl.

3.4. Computational docking of monoterpenoids to the TMD

With a view to establish the determinants of monoterpenoid inhibition of GluCls, each compound was docked to the TMD of SmGluCl-2 and AVR-14B homology models. Dockings were permitted within a large volume that included both the space between helices M1-M4 of a single subunit (“intrasubunit cavity”), equivalent to the binding site for propofol in the crystal structure of the bacterial pLGIC GLIC (Nury et al., 2011), and the space between adjacent subunits (“intersubunit cavity”). All compounds docked preferably to one of two sites within the intersubunit cavity (Fig. 6A and B). Propofol docked preferably to Site 2 in the SmGluCl-2 model, close to the channel-lining M2 helices (Fig. 6C), whereas it docked preferably to Site 1 in the AVR-14B model, further from M2 helices and more directly between M3 and M1 helices from adjacent subunits (Fig. 6D). This difference may be due to the M3 isoleucine side chain in SmGluCl-2 reducing access to Site 1 (orange side chain in Fig. 6C). None of the compounds docked within the intrasubunit cavity, equivalent to the propofol site in the GLIC/propofol crystal structure (Nury et al., 2011), as neither SmGluCl-2 nor AVR-14B models showed a cavity here that was large enough to accommodate any of the monoterpenoids.

Similar patterns were observed for thymol and menthol, with both docking preferentially to Site 1 in the AVR-14B model. For thymol docking to the SmGluCl-2, the five highest ranked dockings yielded similar binding energies, and although the highest ranked was to Site 1 (Fig. 6E), the other four were to Site 2. In fact, in both models, docking poses of each compound were identified at each of the two sites, with the exception of propofol at the AVR-14B model, which docked exclusively to Site 1. That is, most compounds docked with similar predicted free energies (6–7 kcal/mol) to both sites in both channels, but Site 1 was *preferred* in the AVR-14B model and Site 2 was *preferred* in the SmGluCl-2 model, likely

Table 2
Parameters for GluCl inhibition by propofol, thymol and menthol.

	SmGluCl-2				AVR-14B GluCl			
	IC_{50}	n_H	Max. Inhibition[a] (%)	n	IC_{50}	n_H	Max. Inhibition[a] (%)	n
Propofol	1.1 ± 0.4 mM	2.1 ± 0.9	91 ± 2	5	252 ± 48 μM [b]	2.4 ± 0.5[b]	96 ± 1	4[b]
Thymol	484 ± 85 μM	1.6 ± 0.2	95 ± 4	4	1.2 ± 0.2 mM	2.3 ± 0.8	75 ± 5	4
Menthol	[c]	[c]	83 ± 5[d]	3	[c]	[c]	49 ± 9[d]	4

[a] Maximum inhibition of EC_{50} L-glutamate-activated currents.
[b] From (Lynagh and Laube, 2014).
[c] Saturating effect not observed.
[d] Inhibition caused by 10 mM menthol, the highest concentration tested.

due to the SmGluCl-2 M3 isoleucine side chain restricting access to Site 1. The dockings also followed the trend that for each compound, the hydroxyl group was usually oriented towards the M1 helix specifically in the GluCl that was most potently inhibited by that compound. This proximity of the ligand hydroxyl is consistent with the formation of an H-bond with the backbone carbonyl of an M1 residue (alanine in SmGluCl-2, isoleucine in AVR-14B), made available due to the conserved M1 proline four residues downstream (Hibbs and Gouaux, 2011).

4. Discussion

4.1. Agonists in the GluCl ECD

The flatworm SmGluCl-2 and the roundworm AVR-14B share some expected similarities. From the compounds examined, both channels are most potently activated by L-glutamate. This accords with our homology models, showing at the appropriate positions in both receptors the functional side chains that directly interact with bound L-glutamate in the GLC-1 GluCl crystal structure (Hibbs and Gouaux, 2011). There is one key exception, as the Loop G arginine that interacts with the L-glutamate α-carboxyl in AVR-14B is absent from SmGluCl-2, where its functional role is apparently taken over by a Loop A arginine. Amino acid sequence alignments of *S. mansoni* GluCls (Dufour et al., 2013) and also of other trematode transcripts (not shown) suggest that the Loop A arginine is a molecular characteristic of flatworm GluCls. D-glutamate also acts as a full agonist or strong partial agonist at both channels, with 100- and 400-fold lower apparent affinity than L-glutamate at SmGluCl-2 and AVR-14B, respectively. This difference in potencies of L- and D-isomers is quite similar to that seen at tetrameric glutamate-gated cation channels (ionotropic glutamate receptors, iGluRs; (Traynelis et al., 2010)). The full agonism and low millimolar EC_{50} values of L-2-aminoadipic acid at both receptors reflects the similarity in the agonist site of the two GluCls. It is perhaps surprising that this longer compound activates currents as large as those activated by L-glutamate, in contrast to iGluRs, where it is much less efficacious than L-glutamate (Fay et al., 2009). Interestingly, the higher selectivity of AVR-14B for L- over D-glutamate, relative to SmGluCl-2, is continued with an even greater difference for L- over D-2-aminoadipate. Consequently, D-2-aminoadipate is effectively a selective agonist for SmGluCl-2 over AVR-14B GluCls.

The rank order of potency at the AVR-14B of L-glutamate > L-2-aminoadipate > D-glutamate > L-aspartate concurs quite well with the potency of these compounds in inhibiting [^{3}H]L-glutamate binding to the *C. elegans* GLC-1 (Hibbs and Gouaux, 2011), consistent with closely related agonist-binding sites (Fig. 3) in these closely related roundworm GluCls (Beech et al., 2010). Ibotenate (not tested here due to availability) is also a partial agonist at the AVR-14B GluCl, although more potent than the compounds tested here, with an I_{max} equivalent to 69% that of L-glutamate and an EC_{50} only 3-fold higher than L-glutamate (McCavera et al., 2009). Ibotenate contains α-amino and -carboxyl groups, but less like glutamate and more like quisqualate, possesses at the opposite terminal a non-carboxyl, 3-oxyisoxazol group. This indicates that an additional carboxyl group is not an absolute requirement for agonist activity at the AVR-14B GluCl.

In contrast to the AVR-14B GluCl, the SmGluCl-2 was activated up to 28% of the L-glutamate I_{max} by 10 mM quisqualate, the highest molecular weight compound tested. Thus, certain compounds – L-glutamate and L-2-aminoadipate – share the same effects at both GluCls, whereas others – L-aspartate, D-2-aminoadipate, quisqualate and to some extent D-glutamate – are selective for one GluCl or the other. Fig. 3 shows that the architecture of the agonist binding site is quite similar between the two GluCls. Nevertheless, differences such as a longer Loop C and the different position of the positively charged arginine that coordinates the agonist α-carboxyl in the SmGluCl-2 (Fig. 3K) may contribute to differences in agonist specificity. Taken together, these data indicate that agonist pharmacophores in both channels include α-amino and α-carboxyl groups at one terminal of the ligand and carboxyl or other oxygen-containing groups at the opposite terminal of the ligand. Therefore, we speculate that testing further glutamate analogues with alterations to the γ-carboxyl group could reveal numerous agonists of parasite GluCls. Even with the small number of compounds tested here, it is clear that various drugs could selectively activate flatworm or roundworm GluCls, whereas others could activate both and therefore target a broader spectrum of parasites.

Three observations lead us to believe that the L-glutamate binding site in invertebrate GluCls holds promise as an anthelmintic target. Firstly, roundworms and flatworms both possess GluCls at which agonist binding induces robust channel activation. That GluCl channel activation constitutes an effective and a safe anthelmintic mechanism is already established for roundworms (Wolstenholme and Rogers, 2005; Omura, 2008). Although this awaits testing in flatworms, the GluCls of the fluke *S. mansoni* are functionally similar to their roundworm counterparts ((Dufour et al., 2013); present study), and there is evidence for glutamatergic transmission in both tapeworms and flukes (Webb and Eklove, 1989; Webb, 1995b; Brownlee and Fairweather, 1996), admittedly also due to an excitatory, iGluR system (Mendonca-Silva et al., 2002; Taman and Ribeiro, 2011). A notable example of glutamate-like compounds eliciting anthelmintic effects is a decreased tapeworm burden in rats upon a dose of monosodium glutamate (Webb, 1995a), although the means by which this occurs is unknown. Secondly, the structural/chemical landscape of the L-glutamate binding site differs greatly between helminth GluCls on one hand and mammalian receptors for L-glutamate, such as iGluRs and glutamate transporters, on the other. Hibbs and Gouaux (Hibbs and Gouaux, 2011) showed with a *C. elegans* GluCl crystal structure that the α-amino, the α-carboxyl and the γ-carboxyl groups of L-glutamate are distinctly recognized by, respectively: an aromatic box; a positively charged arginine side chain; and a positively charged arginine side chain together with vicinal hydroxyl side chains. Our models suggest a similar site in other roundworm and flatworm GluCls. By contrast, in mammalian iGluRs,

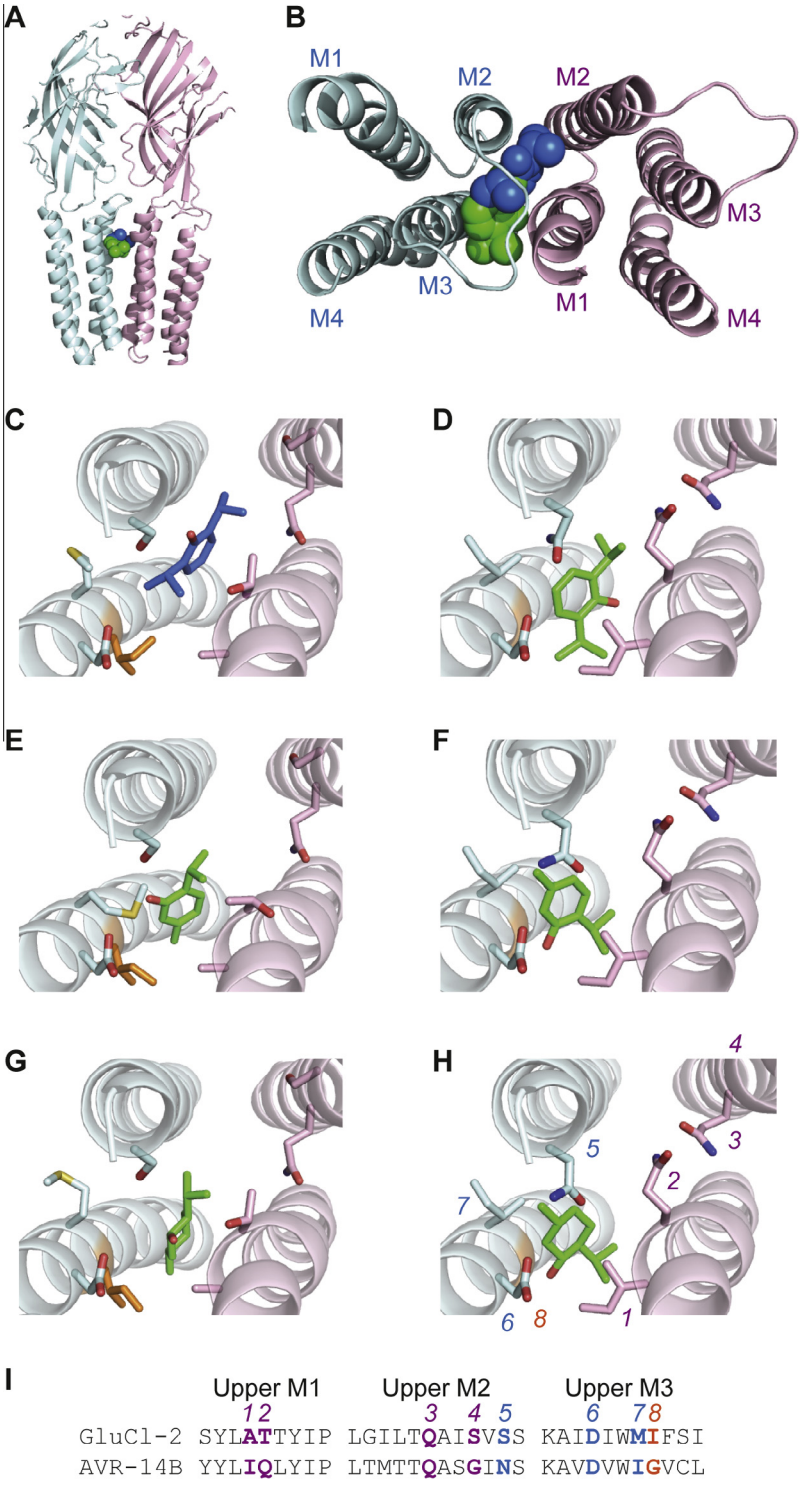

Fig. 6. Simulated dockings to transmembrane domain. (A) Two adjacent subunits of SmGluCl-2 model, viewed from within the membrane plane. Green/blue spheres indicate the vertical level of the sites. (B) Sites 1 (green) and 2 (blue) of the intersubunit cavity are illustrated with spheres. Only the transmembrane helices M1-M4 of adjacent subunits are shown from above. (C-H) Detailed view of inter-subunit cavity in Sm-GluCl-2 (C, E, G) and AVR-14B (D, F, H), showing highest energy dockings of propofol (C and D), thymol (E and F) and menthol (G and H). Color of compound indicates its position in Site 1 or Site 2. Several proximal side chains are indicated and labeled 1–8 in (H) and (I); the alignment of these positions in SmGluCl-2 and AVR-14B subunits is shown in (I). (For interpretation of the references to color in this figure legend, the reader is referred to the web version of this article.)

agonist α-amino, α-carboxyl and γ-carboxyl groups are recognized by, respectively: a negatively charged glutamate or aspartate side chain; a positively charged arginine side chain; and a pair of hydroxyl serine/threonine side chains (Mayer, 2006; Traynelis et al., 2010). Likewise, the make-up of the L-glutamate binding site in mammalian metabotropic glutamate receptors (Kunishima et al., 2000) and glutamate transporters (Yernool et al., 2004) is also very different from that in the GluCl. This implies that helminth GluCls and mammalian L-glutamate receptors likely possess different susceptibility to various other compounds. Thirdly, a handful of

existing insecticides and anthelmintics are pLGIC agonists that kill or disable the parasite via activation of invertebrate acetylcholine receptors (nAChRs; (Harrow and Gration, 1985; Millar and Denholm, 2007)). Given the important role of nAChRs in the human nervous system (Millar and Gotti, 2009) and the relatively subtle differences between invertebrate and mammalian nAChRs (Matsuda et al., 2005), it is remarkable that effective pesticides target the agonist site of invertebrate nAChRs. There are greater differences between invertebrate GluCls and their closest mammalian relatives, GlyRs and $GABA_A$Rs, particularly at the agonist-binding site. Thus, we envisage good prospects for developing GluCl agonists with great selectivity for invertebrate over mammalian receptors.

Finally, we note that both parasite GluCls show rapid desensitization in response to all agonists described. Thus, such compounds do not represent direct replacements for the sustained activation and resulting physiological depression of ivermectin. This does not, however, rule out the future identification of related compounds that bind to the agonist binding site and show less desensitization. Furthermore, compounds binding at this site could be effective by other mechanisms. By binding to the equivalent site to agonists but at a different subunit interface, they may enhance agonist-induced currents, like benzodiazepines at $GABA_A$Rs (Sigel and Buhr, 1997). Conversely, structurally analogous compounds could foreseeably act as competitive antagonists, as is the case at iGluRs (Du et al., 2012). Such drugs could inhibit GluCl signaling and cause hyperexcitability, similar to the common insecticides that block $GABA_A$R ion channels (Bloomquist, 1996). Admittedly, *C. elegans* is reasonably tolerant of GluCl mutations (Dent et al., 2000), suggesting that GluCl antagonists could constitute less effective nematicides than GluCl agonists.

4.2. Modulators in the GluCl TMD

Given the recent demonstration that propofol inhibits the AVR-14B GluCl (Lynagh and Laube, 2014), it is perhaps not surprising that it also inhibits the SmGluCl-2. The potency was, however, some 4-fold lower at the SmGluCl-2. Based on our docking of propofol to homology models, this difference may be due to an M3 isoleucine residue in the SmGluCl-2 that prevents propofol from accessing exactly the same site as in the AVR-14B (site 1, between M3 and M1 helices of adjacent subunits), and restricts the propofol molecule to site 2 (between adjacent subunits but closer to M2 helices). This is in strict accord with mutagenesis data, where an M3 glycine-isoleucine mutation reduces propofol sensitivity of the AVR-14B GluCl (Lynagh and Laube, 2014).

Thymol, which differs from propofol in that the 6-isopropyl group is replaced by a 5-methyl group, inhibited the SmGluCl-2 with higher potency than propofol but inhibited the AVR-14B with lower potency than propofol. In our dockings to the SmGluCl-2 model, the poses of propofol and thymol were generally similar, occupying in most cases site 2 (with the exception of the highly-ranked pose of thymol in close proximity to M3 in site 1; Fig. 6E). The major difference between the ligands appears to be the orientation of the ligand hydroxyl, which in most poses oriented towards M1 for the more potent ligand, thymol, such that it can form an H-bond with a backbone carbonyl made available by the conserved M1 proline (Hibbs and Gouaux, 2011). Similarly, in the AVR-14B model, the phenyl ring of both ligands occupies site 1, but the hydroxyl is oriented towards the same M1 backbone carbonyl specifically in the case of propofol, the more potent inhibitor of AVR-14B. Hydrogen-bonding to the backbone carbonyl of this GluCl M1 position has also been demonstrated for ivermectin (Hibbs and Gouaux, 2011), although the latter occupies a much larger volume, makes numerous other interactions and enhances channel gating (Hibbs and Gouaux, 2011). Our dockings suggest no reason for the lower potency of the non-phenyl ligand menthol, as its location and orientation in both models appears nearly identical to thymol. We are also at a loss to explain the small enhancement by thymol of the sustained current at AVR-14B (section 3.3, above). However, whether monoterpenoid binding inclines the agonist-bound channel towards a closed or open state is quite susceptible to structural alterations in the TMD (Lynagh and Laube, 2014); it is easy to imagine that thymol binding to structurally distinct resting, open or desensitized AVR-14B channels could exert opposing effects, manifest in inhibition of peak currents but small enhancement of sustained/desensitized currents.

Given the effects on monoterpenoid sensitivity of mutations (Lynagh and Laube, 2014) or naturally occurring differences (present study) at the GluCl M3 position, together with the fact that all compounds docked to either site 1 or 2 between adjacent subunits (and not once to a possible site within individual subunits), we conclude that the intersubunit cavity of the GluCl TMD is the most likely binding site for monoterpenoids. It should be noted that this cavity may be artificially enlarged in our models due to the presence of bound ivermectin in the template GLC-1 structure. (Each of the four available GLC-1 crystal structures include ivermectin (Hibbs and Gouaux, 2011); we have utilized the one complexed with L-glutamate.) Nevertheless, inspection of the GLC-1 structure and residue conservation within GluCls suggest that there is unlikely to be a plausible intrasubunit cavity that can bind monoterpenoids, as exists in cation-selective pLGICs (Nury et al., 2011). Both intersubunit sites 1 and 2 are also in close proximity to the M2 15′ residue, a determinant of propofol sensitivity in $GABA_A$Rs and GlyRs (Pistis et al., 1999; Siegwart et al., 2003; Ahrens et al., 2008), and the M2 17′ residue that binds *ortho*-propofol diazirine in $GABA_A$Rs (Yip et al., 2013). In fact, one isopropyl group of propofol is oriented directly towards the M2 17′ serine residue in SmGluCl-2 (position 4 in Fig. 6I) that equates to the M2 histidine residue in $GABA_A$Rs that binds the diazirine of *ortho*-propofol diazirine (Yip et al., 2013).

Propofol is widely used for its anesthetic effects, which are likely mediated via its enhancement of $GABA_A$Rs and GlyRs (Franks and Lieb, 1994; Nguyen et al., 2009). Thymol is a naturally occurring compound that also enhances $GABA_A$Rs, both of the heteromeric human and homomeric *Drosophila melanogaster* isoforms (Priestley et al., 2003). We think monoterpenoids hold promise for the development of potent GluCl modulators for the following reasons. Firstly, chemical fine-tuning of potency and selectivity of such compounds has already been demonstrated. For example, halogenation of the C4 position of propofol leads to remarkable increases in potency at mammalian α1 GlyRs (de la Roche et al., 2012), has little effect on potency at mammalian $\alpha1\beta1\gamma2$ $GABA_A$Rs (Trapani et al., 1998), and decreases potency at mammalian $\alpha1\beta2\gamma2$ $GABA_A$Rs (Krasowski et al., 2001). Secondly, binding sites between subunits occur in both roundworm and flatworm GluCls. This is remarkable when compared to ivermectin, whose inactivity at flatworms is due to molecular differences at this very site (Lynagh and Lynch, 2012a; Dufour et al., 2013). It is doubtful that this particular site could be targeted by a single drug of a broad helminth spectrum, however, as differential potency at roundworm vs. flatworm GluCls seems common to these modulators. Finally, numerous monoterpenoids, with similar structures and properties to the compounds examined here, occur naturally. Thus, nature provides a large number of compounds that could be tested for potent modulation of GluCls. On this note, it is intriguing that several such compounds (including thymol and menthol), or the plants from which they derive, are toxic to *H. contortus* (Carvalho et al., 2012; Boubaker Elandalousi et al., 2013; Zhu et al., 2013), although it is pure speculation that this toxicity could involve GluCls.

4.3. Conclusions

This study reveals that a flatworm and a roundworm GluCl harbor binding sites in the extracellular domain for agonists related to L-glutamate but of notable differences in size and functional groups. Furthermore, it shows that both of these GluCls also harbor a transmembrane cavity to which monoterpenoids bind and inhibit channel activation by L-glutamate. Each agonist or modulator examined was of relatively low potency – high micromolar and low millimolar concentrations are required for efficient channel modulation or activation, respectively – rendering them unsuitable for anthelmintic use. However, we propose that subtly divergent compounds could exert similar effects but with much greater potency and thus provide leads for the development of much-needed drugs against schistosomiasis. Furthermore, as the extracellular site shows significant pharmacological similarity between flatworm and roundworm GluCls, drugs targeting this site could constitute anthelmintics of a very broad spectrum.

Acknowledgements

The authors are grateful to Professor Timothy G. Geary of (McGill University) for the donation of the SmGluCl-2 clone and to Professor Adrian J. Wolstenholme (University of Georgia) for the donation of the AVR-14B clone. The authors declare no conflicts of interest.

References

Ahrens, J., Leuwer, M., Stachura, S., Krampfl, K., Belelli, D., Lambert, J.J., et al., 2008. A transmembrane residue influences the interaction of propofol with the strychnine-sensitive glycine alpha1 and alpha1beta receptor. Anesth. Analg. 107 (6), 1875–1883.

Beech, R.N., Wolstenholme, A.J., Neveu, C., Dent, J.A., 2010. Nematode parasite genes: what's in a name? Trends Parasitol 26 (7), 334–340.

Bloomquist, J.R., 1996. Ion channels as targets for insecticides. Annu. Rev. Entomol. 41, 163–190.

Botros, S., Pica-Mattoccia, L., William, S., El-Lakkani, N., Cioli, D., 2005. Effect of praziquantel on the immature stages of *Schistosoma haematobium*. Int. J. Parasitol. 35 (13), 1453–1457.

Boubaker Elandalousi, R., Akkari, H., B'Chir, F., Gharbi, M., Mhadhbi, M., Awadi, S., et al., 2013. *Thymus capitatus* from Tunisian arid zone: chemical composition and in vitro anthelmintic effects on *Haemonchus contortus*. Vet. Parasitol. 197 (1–2), 374–378.

Brownlee, D.J., Fairweather, I., 1996. Immunocytochemical localization of glutamate-like immunoreactivity within the nervous system of the cestode *Mesocestoides corti* and the trematode *Fasciola hepatica*. Parasitol. Res. 82 (5), 423–427.

Caffrey, C.R., Secor, W.E., 2011. Schistosomiasis: from drug deployment to drug development. Curr. Opin. Infect. Dis. 24 (5), 410–417.

Campbell, W.C., Fisher, M.H., Stapley, E.O., Albers-Schonberg, G., Jacob, T.A., 1983. Ivermectin: a potent new antiparasitic agent. Science 221 (4613), 823–828.

Carvalho, C.O., Chagas, A.C., Cotinguiba, F., Furlan, M., Brito, L.G., Chaves, F.C., et al., 2012. The anthelmintic effect of plant extracts on *Haemonchus contortus* and *Strongyloides venezuelensis*. Vet. Parasitol. 183 (3–4), 260–268.

de la Roche, J., Leuwer, M., Krampfl, K., Haeseler, G., Dengler, R., Buchholz, V., et al., 2012. 4-Chloropropofol enhances chloride currents in human hyperekplexic and artificial mutated glycine receptors. BMC Neurol. 12, 104.

Dent, J.A., 2006. Evidence for a diverse Cys-loop ligand-gated ion channel superfamily in early bilateria. J. Mol. Evol. 62 (5), 523–535.

Dent, J.A., Smith, M.M., Vassilatis, D.K., Avery, L., 2000. The genetics of ivermectin resistance in *Caenorhabditis elegans*. Proc. Natl. Acad. Sci. U.S.A. 97 (6), 2674–2679.

Doenhoff, M.J., Cioli, D., Utzinger, J., 2008. Praziquantel: mechanisms of action, resistance and new derivatives for schistosomiasis. Curr. Opin. Infect. Dis. 21 (6), 659–667.

Du, J., Dong, H., Zhou, H.X., 2012. Size matters in activation/inhibition of ligand-gated ion channels. Trends Pharmacol. Sci. 33 (9), 482–493.

Dufour, V., Beech, R.N., Wever, C., Dent, J.A., Geary, T.G., 2013. Molecular cloning and characterization of novel glutamate-gated chloride channel subunits from *Schistosoma mansoni*. PLoS Pathog. 9 (8), e1003586.

Eswar, N., Webb, B., Marti-Renom, M.A., Madhusudhan, M.S., Eramian, D., Shen, M.Y. et al. (2006). Comparative protein structure modeling using Modeller. Current protocols in bioinformatics/editorial board, Andreas D. Baxevanis et al. Chapter 5: Unit 5 6.

Fay, A.M., Corbeil, C.R., Brown, P., Moitessier, N., Bowie, D., 2009. Functional characterization and in silico docking of full and partial GluK2 kainate receptor agonists. Mol. Pharmacol. 75 (5), 1096–1107.

Franks, N.P., Lieb, W.R., 1994. Molecular and cellular mechanisms of general anaesthesia. Nature 367 (6464), 607–614.

Glendinning, S.K., Buckingham, S.D., Sattelle, D.B., Wonnacott, S., Wolstenholme, A.J., 2011. Glutamate-gated chloride channels of *Haemonchus contortus* restore drug sensitivity to ivermectin resistant *Caenorhabditis elegans*. PLoS ONE 6 (7), e22390.

Gryseels, B., Mbaye, A., De Vlas, S.J., Stelma, F.F., Guisse, F., Van Lieshout, L., et al., 2001. Are poor responses to praziquantel for the treatment of *Schistosoma mansoni* infections in Senegal due to resistance? An overview of the evidence. Trop. Med. Int. Health 6 (11), 864–873.

Gryseels, B., Polman, K., Clerinx, J., Kestens, L., 2006. Human schistosomiasis. Lancet 368 (9541), 1106–1118.

Harrow, I.D., Gration, K.A.F., 1985. Mode of action of the anthelmintics morantel, pyrantel and levamisole on muscle-cell membrane of the nematode *Ascaris suum*. Pestic. Sci. 16 (6), 662–672.

Hibbs, R.E., Gouaux, E., 2011. Principles of activation and permeation in an anion-selective Cys-loop receptor. Nature 474 (7349), 54–60.

Kass, I.S., Wang, C.C., Walrond, J.P., Stretton, A.O., 1980. Avermectin B1a, a paralyzing anthelmintic that affects interneurons and inhibitory motoneurons in *Ascaris*. Proc. Natl. Acad. Sci. U.S.A. 77 (10), 6211–6215.

King, C.H., 2010. Parasites and poverty: the case of schistosomiasis. Acta Trop. 113 (2), 95–104.

King, C.H., Dickman, K., Tisch, D.J., 2005. Reassessment of the cost of chronic helmintic infection: a meta-analysis of disability-related outcomes in endemic schistosomiasis. Lancet 365 (9470), 1561–1569.

Krasowski, M.D., Jenkins, A., Flood, P., Kung, A.Y., Hopfinger, A.J., Harrison, N.L., 2001. General anesthetic potencies of a series of propofol analogs correlate with potency for potentiation of gamma-aminobutyric acid (GABA) current at the GABA(A) receptor but not with lipid solubility. J. Pharmacol. Exp. Ther. 297 (1), 338–351.

Kunishima, N., Shimada, Y., Tsuji, Y., Sato, T., Yamamoto, M., Kumasaka, T., et al., 2000. Structural basis of glutamate recognition by a dimeric metabotropic glutamate receptor. Nature 407 (6807), 971–977.

Larkin, M.A., Blackshields, G., Brown, N.P., Chenna, R., McGettigan, P.A., McWilliam, H., et al., 2007. Clustal W and Clustal X version 2.0. Bioinformatics 23 (21), 2947–2948.

Lynagh, T., Laube, B., 2014. Opposing effects of the anesthetic propofol at pentameric ligand-gated ion channels mediated by a common site. J. Neurosci. 34 (6), 2155–2159.

Lynagh, T., Lynch, J.W., 2012a. Ivermectin binding sites in human and invertebrate Cys-loop receptors. Trends Pharmacol. Sci. 33 (8), 432–441.

Lynagh, T., Lynch, J.W., 2012b. Molecular mechanisms of Cys-loop ion channel receptor modulation by ivermectin. Front. Mol. Neurosci. 5, 60.

Lynagh, T., Kunz, A., Laube, B., 2013. Propofol modulation of alpha1 glycine receptors does not require a structural transition at adjacent subunits that is crucial to agonist-induced activation. ACS Chem. Neurosci. 4 (11), 1469–1478.

Matsuda, K., Shimomura, M., Ihara, M., Akamatsu, M., Sattelle, D.B., 2005. Neonicotinoids show selective and diverse actions on their nicotinic receptor targets: electrophysiology, molecular biology, and receptor modeling studies. Biosci. Biotechnol. Biochem. 69 (8), 1442–1452.

Mayer, M.L., 2006. Glutamate receptors at atomic resolution. Nature 440 (7083), 456–462.

McCavera, S., Rogers, A.T., Yates, D.M., Woods, D.J., Wolstenholme, A.J., 2009. An ivermectin-sensitive glutamate-gated chloride channel from the parasitic nematode *Haemonchus contortus*. Mol. Pharmacol. 75 (6), 1347–1355.

Mendonca-Silva, D.L., Pessoa, R.F., Noel, F., 2002. Evidence for the presence of glutamatergic receptors in adult *Schistosoma mansoni*. Biochem. Pharmacol. 64 (9), 1337–1344.

Millar, N.S., Denholm, I., 2007. Nicotinic acetylcholine receptors: targets for commercially important insecticides. Invert. Neurosci. 7 (1), 53–66.

Millar, N.S., Gotti, C., 2009. Diversity of vertebrate nicotinic acetylcholine receptors. Neuropharmacology 56 (1), 237–246.

Moreno, Y., Nabhan, J.F., Solomon, J., Mackenzie, C.D., Geary, T.G., 2010. Ivermectin disrupts the function of the excretory-secretory apparatus in microfilariae of *Brugia malayi*. Proc. Natl. Acad. Sci. U.S.A. 107 (46), 20120–20125.

Nguyen, H.T., Li, K.Y., daGraca, R.L., Delphin, E., Xiong, M., Ye, J.H., 2009. Behavior and cellular evidence for propofol-induced hypnosis involving brain glycine receptors. Anesthesiology 110 (2), 326–332.

Nury, H., Van Renterghem, C., Weng, Y., Tran, A., Baaden, M., Dufresne, V., et al., 2011. X-ray structures of general anaesthetics bound to a pentameric ligand-gated ion channel. Nature 469 (7330), 428–431.

Omura, S., 2008. Ivermectin: 25 years and still going strong. Int. J. Antimicrob. Agents 31 (2), 91–98.

Perez-Serrano, J., Grosman, C., Urrea-Paris, M.A., Denegri, G., Casado, N., Rodriguez-Caabeiro, F., 2001. Depolarization of the tegument precedes morphological alterations in *Echinococcus granulosus* protoscoleces incubated with ivermectin. Parasitol. Res. 87 (10), 804–807.

Perry, R.N., 2001. Analysis of the sensory responses of parasitic nematodes using electrophysiology. Int. J. Parasitol. 31 (9), 909–918.

Pica-Mattoccia, L., Cioli, D., 2004. Sex- and stage-related sensitivity of *Schistosoma mansoni* to in vivo and in vitro praziquantel treatment. Int. J. Parasitol. 34 (4), 527–533.

Pistis, M., Belelli, D., McGurk, K., Peters, J.A., Lambert, J.J., 1999. Complementary regulation of anaesthetic activation of human (alpha6beta3gamma2L) and Drosophila (RDL) GABA receptors by a single amino acid residue. J. Physiol. 515 (Pt 1), 3–18.

Priestley, C.M., Williamson, E.M., Wafford, K.A., Sattelle, D.B., 2003. Thymol, a constituent of thyme essential oil, is a positive allosteric modulator of human GABA(A) receptors and a homo-oligomeric GABA receptor from *Drosophila melanogaster*. Br. J. Pharmacol. 140 (8), 1363–1372.

Shoop, W.L., Ostlind, D.A., Rohrer, S.P., Mickle, G., Haines, H.W., Michael, B.F., et al., 1995. Avermectins and milbemycins against *Fasciola hepatica*: in vivo drug efficacy and in vitro receptor binding. Int. J. Parasitol. 25 (8), 923–927.

Siegwart, R., Krahenbuhl, K., Lambert, S., Rudolph, U., 2003. Mutational analysis of molecular requirements for the actions of general anaesthetics at the gamma-aminobutyric acidA receptor subtype, alpha1beta2gamma2. BMC Pharmacol. 3, 13.

Sigel, E., Buhr, A., 1997. The benzodiazepine binding site of GABAA receptors. Trends Pharmacol. Sci. 18 (11), 425–429.

Taman, A., Ribeiro, P., 2011. Glutamate-mediated signaling in *Schistosoma mansoni*: a novel glutamate receptor is expressed in neurons and the female reproductive tract. Mol. Biochem. Parasitol. 176 (1), 42–50.

Thetiot-Laurent, S.A., Boissier, J., Robert, A., Meunier, B., 2013. Schistosomiasis chemotherapy. Angew. Chem. Int. Ed. Engl. 52 (31), 7936–7956.

Tong, F., Coats, J.R., 2012. Quantitative structure-activity relationships of monoterpenoid binding activities to the housefly GABA receptor. Pest Manag. Sci. 68 (8), 1122–1129.

Trapani, G., Latrofa, A., Franco, M., Altomare, C., Sanna, E., Usala, M., et al., 1998. Propofol analogues. Synthesis, relationships between structure and affinity at GABAA receptor in rat brain, and differential electrophysiological profile at recombinant human GABAA receptors. J. Med. Chem. 41 (11), 1846–1854.

Traynelis, S.F., Wollmuth, L.P., McBain, C.J., Menniti, F.S., Vance, K.M., Ogden, K.K., et al., 2010. Glutamate receptor ion channels: structure, regulation, and function. Pharmacol. Rev. 62 (3), 405–496.

Trott, O., Olson, A.J., 2010. AutoDock Vina: improving the speed and accuracy of docking with a new scoring function, efficient optimization, and multithreading. J. Comput. Chem. 31 (2), 455–461.

van der Werf, M.J., de Vlas, S.J., Brooker, S., Looman, C.W., Nagelkerke, N.J., Habbema, J.D., et al., 2003. Quantification of clinical morbidity associated with schistosome infection in sub-Saharan Africa. Acta Trop. 86 (2–3), 125–139.

Webb, R.A., 1995a. An acute dose of monosodium L-glutamate causes decreased fecundity and enhanced loss of the cestode *Hymenolepis diminuta* from rats. Parasitol. Res. 81 (3), 202–206.

Webb, R.A., 1995b. Electrical field-stimulated release of L-[G-3H]-glutamate from tissue slices of the cestode *Hymenolepis diminuta*. Parasitol. Res. 81 (2), 173–174.

Webb, R.A., Eklove, H., 1989. Demonstration of intense glutamate-like immunoreactivity in the longitudinal nerve cords of the cestode *Hymenolepis diminuta*. Parasitol. Res. 75 (7), 545–548.

Wolstenholme, A.J., 2012. Glutamate-gated chloride channels. J. Biol. Chem. 287 (48), 40232–40238.

Wolstenholme, A.J., Rogers, A.T., 2005. Glutamate-gated chloride channels and the mode of action of the avermectin/milbemycin anthelmintics. Parasitology 131 (Suppl.), S85–95.

Yernool, D., Boudker, O., Jin, Y., Gouaux, E., 2004. Structure of a glutamate transporter homologue from *Pyrococcus horikoshii*. Nature 431 (7010), 811–818.

Yip, G.M., Chen, Z.W., Edge, C.J., Smith, E.H., Dickinson, R., Hohenester, E., et al., 2013. A propofol binding site on mammalian GABA receptors identified by photolabeling. Nat. Chem. Biol.

Zhu, L., Dai, J., Yang, L., Qiu, J., 2013. Anthelmintic activity of *Arisaema franchetianum* and *Arisaema lobatum* essential oils against *Haemonchus contortus*. J. Ethnopharmacol. 148 (1), 311–316.